第33卷 第6期 焊 接 学 报 Vol. 33 No. 6
2012年6月 TRANSACTIONS OF THE CHINA WELDING INSTITUTION June 2012

CLAM 钢激光焊 T 形接头残余应力及硬度分析

雷玉成[1]， 李振南[1]， 朱延山[2]， 巨 新[3]
(1. 江苏大学 材料科学与工程学院，镇江 212013; 2. 济南钢铁股份有限公司技术中心，济南 250101;
3. 北京科技大学 数理学院，北京 100083)

摘 要: 采用功率为 4 kW 的 Nd: YAG 激光器，对 4 mm 厚的 CLAM 钢板组成的 T 形接头，用不同的激光入射角度进行了激光焊接试验，对焊缝接头的宏观成形，残余应力的分布以及硬度变化进行观察和测试. 结果表明，入射角度为 14°时焊缝接头具有明显的未熔合现象，随着焊接角度的减小，采用 12°和 10°时完全熔合，接头表面的残余应力为压应力，入射角度为 12°时翼板残余压应力比腹板的大，入射角度为 10°时腹板的残余应力较大，接头截面的内部残余应力变化很大，焊缝区的硬度相对于母材有明显提高，焊接热影响区未出现软化现象.

关键词: 中国低活化马氏体钢; Nd: YAG 激光焊; 入射角度; 残余应力; 硬度
中图分类号: TG456.7 文献标识码: A 文章编号: 0253-360X(2012)06-0073-04

雷玉成

0 序 言

核聚变能被认为是满足人类未来能源需求的潜在技术，将有可能成为最终解决人类能源问题的主要途径. 由于低活化铁素体/马氏体钢(reduced activation ferritic/martensitic, RAFM)和奥氏体不锈钢相比，在强辐照下具有固有的几何稳定性、低的线膨胀系数、高热导率等优良的热物理特性，且其低活化成分适于商业化生产，被认为是极具潜力的聚变堆候选结构材料. 这里指出，所谓的低活化材料其含意是经过若干年辐照后其放射性元素主要来自于短寿命或中等寿命放射性元素的材料. 这样，合金材料经过 300 年后其放射性水平能够满足手工处置条件. 中国低活化马氏体钢(China low activation martensitic, CLAM)是具有中国自主知识产权的成分及性能优化的 RAFM 钢[1].

由于激光焊能够将激光束集中于非常狭小的区域，从而产生高能量密度的热源，具有能量集中、焊缝及热影响区(HAZ)窄、深宽比大、生产效率高、制造精度高等许多优点，因此 RAFM 钢激光焊接研究也成为聚变堆包层结构制造的重要课题[2,3]. 聚变堆包层结构十分复杂，内壁、隔板等许多部件中均含有各种尺寸和形状的小口径流道，在焊接这些结构时由于可操作空间狭小，焊枪无法进入到待焊部位，致使许多常规焊接方法无法进行[2]. 而激光焊由于光束集中，可以通过小角度焊接的方法到达待焊部位，最终获得成形良好的焊缝. 可见研究小角度激光自动焊接技术对于推动聚变堆结构制造技术有着十分重要的实际意义和理论价值.

文中采用激光焊接方法进行 CLAM 钢 T 形接头的小角度焊接，焊接完成后取部分试样分别测定其腹板和翼板的纵向和横向残余应力，对其硬度和微观组织结构进行测试和观察.

1 试验方法

试验所用材料为 12 mm 厚的 CALM 钢板，热处理工艺为 980 ℃/30 min，水冷淬火，然后 760 ℃/90 min 回火处理，CLAM 钢的化学成分见表 1. 微观组织为板条马氏体，在晶内和晶界分布着尺寸大约为 30~100 nm 起弥散强化作用的析出碳化物，主要为 $M_{23}C_6$[3,4].

表 1 CLAM 钢的化学成分(质量分数，%)
Table 1 Chemical compositions of CLAM

Cr	W	V	Ta	Mn	C	S	Si
8.91	1.44	0.20	0.15	0.35	0.12	0.003	0.065
O	N	Co	Cu	Al	Ti	Ni	Fe
0.002	0.008 4	0.006	0.028	0.18	0.004	0.043	余量

收稿日期: 2011-04-18
基金项目: 江苏省研究生创新计划资助项目(CX09B_195Z); 国家973 计划资助项目(2008CB717802)

将12 mm厚的板材经线切割加工成厚度为4 mm的薄板，T形接头的腹板尺寸为30 mm×30 mm×4 mm，翼板尺寸为30 mm×60 mm×4 mm.

试验使用德国TRUMPF公司的HL4006D Nd:YAG激光器，最大功率为4 kW. 采用单侧焊接的方法. 选取3组焊接试样，分别采取不同的激光入射角度进行激光焊接，试验工艺参数如表2所示.

表2 激光焊接工艺参数

Table 2 Process parameters of laser welding

试样	焦距 f_c/mm	焊接速度 v/(m·min^{-1})	功率 P/kW	激光入射角度 θ/(°)
1	200	1.0	4	14
2	200	1.0	4	12
3	200	1.0	4	10

采用X射线应力测定仪测定残余应力，先测定平行于焊缝方向的横向残余应力，然后从试样上沿垂直于焊缝的方向切去5 mm，再对其截面分别进行残余应力测试，硬度测试和宏观分析. 硬度测试采用HVS-1000型显微硬度计. 宏观分析试样浸蚀液为盐酸、苦味酸和酒精的混合溶液，其中盐酸含量为5 mL，酒精含量为95 mL，在盐酸酒精混合液中加入5 g的苦味酸.

2 试验结果与分析

2.1 宏观分析

焊后观察3组试样焊缝的外观，其截面如图1所示，从宏观上看，1号试样由于激光入射角度相对2号，3号试样偏大，激光束能量更多偏向翼板，无法穿透腹板，其焊缝存在明显的未焊透现象. 2号，3号试样激光入射角度较小，完全熔合，焊缝光滑且均匀连续，焊缝细，HAZ窄，由于3号试样角度相对2号更小，能量更易穿过腹板，其腹板未焊接侧焊缝较长.

2.2 残余应力测试

对1～3号试样进行残余应力测定，测定角为0°，25°，35°，45°. 应力常数为-318 MPa/(°) 由于1号试样明显未焊透，因此文中只测定2号，3号的残余应力. 分别测试焊缝截面的残余应力和沿焊缝方向的横向残余应力，将平行于y轴的残余应力定义为应力σ_y，平行于x轴的残余应力方向定义为σ_x，平行于z轴的残余应力方向定义为σ_z. 为了便于分析应力，定起弧位置为坐标原点，图2为应力测试路径，具体位置在表3中列出. 图3为各条路径上具体位置的应力测试值.

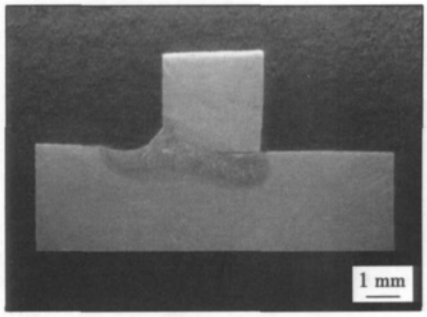

(a) 试样1焊接接头横截面

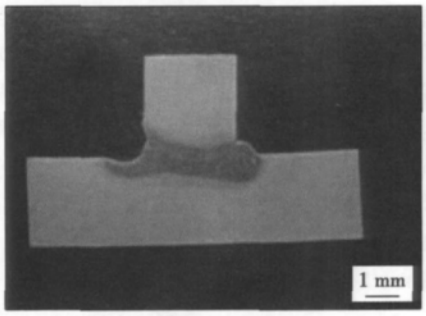

(b) 试样2焊接接头横截面

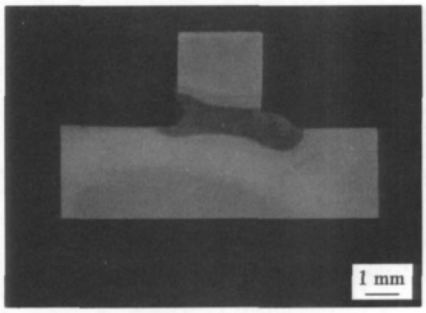

(c) 试样3焊接接头横截面

图1 焊缝接头截面宏观形貌

Fig. 1 Cross-sections of weld joint

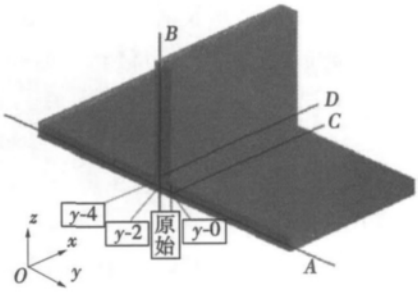

图2 残余应力标记

Fig. 2 Market place of residual stress

表3 应力测试路径位置

Table 3 Positions of stress test path

应力测试路径	应力测试位置
A	$y\in(-9,5)$，$x=6$，$z=-1$
B	$y=-2$，$x=6$，$z\in(-4,4)$
C	$y=1$，$x\in(0,30)$，$z=0$
D	$y=0$，$x\in(0,30)$，$z=1$

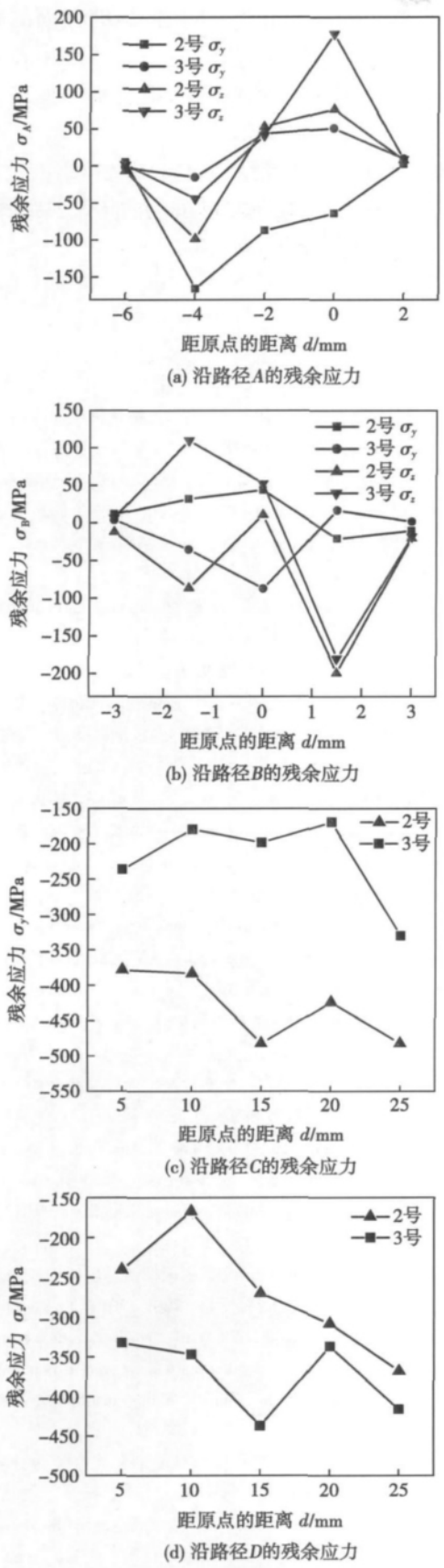

图 3　不同路径下残余应力分布

Fig. 3　Distribution of residual stress with different paths

在测定 T 形焊缝表面的残余应力时，反射后产生的干涉条纹无法在回转膜上形成干涉环，因此无法测量纵向残余应力，只可以测定其横向残余应力[5]．从图 3a，b 中可以看到，由于焊接残余应力是自身平衡的内力[6]，在焊接截面的焊接残余应力随着测试位置的不同变化是很大的，残余应力不仅大小发生变化，方向也会发生变化．靠近熔池底部的残余应力较大，随着不断的远离熔深区域，残余应力逐渐减小．在图 3a 中，2 号试样残余应力 σ_y 以压应力为主，3 号试样的 σ_y 以拉应力为主．同时 2 号试样的残余应力 σ_y 的绝对值大于 3 号试样．这是因为对于翼板来说，角度愈大，在焊接时受到的热量越多，残余应力越大．图 3c 与图 3d 也说明了焊接角度与腹板翼板残余应力的关系，激光入射角度较大时，翼板残余应力较大，激光入射角度较小时，腹板残余应力较大．图 3a 中的残余应力 σ_z 因为要受到 σ_y 的影响，结果比较复杂，既有拉应力又有压应力，在 $y=-2$ 和 $y=0$ 处为拉应力，$y=-4$ 处为压应力，从 $y=-4$ 到原点残余应力的总体趋势是残余压应力不断减小，逐渐向拉应力过渡．这是由于熔池冷却凝固过程的热量主要是通过基材导出的[7]．$y=0$ 处温度最高，冷却最晚，熔池底部 $y=-4$ 处温度最低，冷却最早，由于先冷却的区域低于塑性温度时，后冷却的还处于塑性状态，当该区域继续冷却时，其收缩受到已凝固区域的阻碍，从而先凝固区域承受压应力，后凝固区域受到拉应力[8]．图 3*b* 中，$z>0$ 处为腹板的残余应力，$z<0$ 为翼板的残余应力．残余应力 σ_y 的变化比较小，最大应力值出现在原点，而残余应力 σ_z 的变化明显，最大值出现在 $x=1.5$ 处，即出现在腹板上．残余应力 σ_z 的数值明显大于残余应力 σ_y，这是因为试样在焊接时，在 z 轴方向需要固定，夹具会给试样很大的拘束力，导致残余应力变大．

2.3　硬度测试与分析

沿图 3 中的路径 A，B 对焊接接头的横截面进行硬度测试．载荷 9.8 N，加载时间为 15 s．图 4 为 2 号试样焊缝处金相组织形貌．分别对 2，3 号试样测得了焊缝、热影响区和母材的维氏硬度，横截面上测试的硬度值如图 5 所示．

由图 5 可见，焊接角度的变化对于焊缝和热影响区的硬度没有太大的影响．母材平均硬度为 221 HV 左右；热影响区硬度在 348 ~ 398 HV；焊缝区在 389 ~ 462 HV，明显高于母材的平均硬度，焊缝出现了明显的硬化现象．这是因为焊缝区和附近热影响区得到硬度偏高的粗大板条马氏体组织（图 4）．靠近母材的热影响区，受焊接热循环的作用，温度在 A_{c_3} 以下（大部分在 A_{c_1} 附近），相当于经历了一次回

火，导致硬度略微下降.

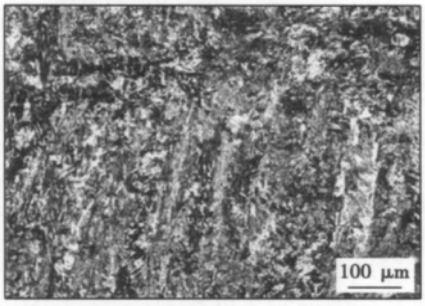

图4 2号试样焊缝金相组织形貌

Fig. 4 Optical micrograph of weld metal of No. 2

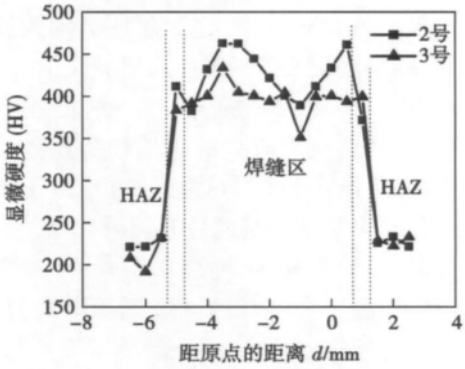

(a) 沿路径A的焊接接头硬度

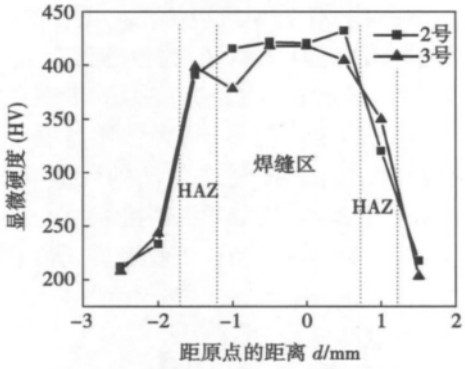

(b) 沿路径B的焊接接头硬度

图5 接头显微硬度

Fig. 5 Hardness distribution

3 结 论

(1) 不同激光入射角度对焊缝的成形影响很大，选择合适的入射角度可以保证焊缝的成形良好. 14°时，接头会产生明显未熔合现象，而入射角度为12°和10°时，可以获得成形良好的焊接接头.

(2) 残余应力的大小与激光的入射角度有很大关系，焊接角度较大时翼板的残余应力较大，角度较小时腹板的残余应力较大. 同时，焊缝截面的残余应力大小和方向均发生变化，应力主要集中在焊缝和热影响区，沿焊缝方向的残余应力均为压应力且数值很大，最大值可达487 MPa.

(3) 焊接接头的硬度与母材硬度相比出现了明显的硬化现象，几乎是母材硬度的两倍，但接头的硬度与激光的入射角度大小无关.

参考文献:

[1] 雷玉成，韩明娟，朱 强，等. 中国低活化钢激光焊接接头微观组织与硬度分析 [J]. 焊接学报，2010，31(1)：5－8.
Lei Yucheng，Han Mingjuan，Zhu Qiang，*et al*. Microstructure and hardness of laser welded joint of China low activation martensitic steel [J]. Transactions of the China Welding Institution，2010，31(1)：5－8.

[2] Yin Z S，Kim S H，Hai D C，*et al*. Precipitate phase of a ferritic/martensitic 9% Cr steel for nuclear power reactor [J]. Nuclear Engineering and Design，2009，239：648－654.

[3] 雷玉成，张 玲，顾康家，等. 中国低活马氏体钢TIG焊温度场接头组织分析 [J]. 江苏大学学报(自然科学版)，2009，30(5)：479－482.
Lei Yucheng，Zhang Ling，Gu Kangjia，*et al*. Analysis of temperature field and joint microstructures on China low activation martensitic steel TIG weld [J]. Journal of Jiangsu University(Natural Science Edition)，2009，30(5)：479－482.

[4] Huang Q，Li C. Process in development of China low activation martensitic steel for fusion application [J]. Journal of Nuclear Materials，2007，3(153)：1－5.

[5] 宋天民. 焊接残余应力的产生与消除 [M]. 北京：中国石化出版社，2005.

[6] 江克斌，肖叶桃，郭永涛，T型焊接试件焊接残余应力分布的测定 [J]. 焊接学报，2008，29(1)；53－59.
Jiang Kebin，Xiao Yetao，Guo Yongtao. Determination of welding residual stress distribution in T-shape welded specimen [J]. Transactions of the China Welding Institution，2008，9(1)：53－59.

[7] 雷玉成，顾康家，朱 强，等. 中国低活马氏体钢融化焊接头硬度与微观组织 [J]. 焊接学报，2009，30(11)：9－11.
Lei Yucheng，Gu Kangjia，Zhu Qiang，*et al*. Hardness and microstructure of China low activation martensitic steel fusion weld joint [J]. Transactions of the China Welding Institution，2009，30(11)：9－11.

[8] 张喜梅，张世联. T型材角接焊的变形和残余应力分析 [J]. 舰船科学技术，2008，30(3)；72－77.
Zhang Ximei，Zhang Shilian，*et al*. Analysis of the deformation and residual stress of T-joint fillet weld [J]. Ship Science And Technology，2008，30(3)：72－77.

作者简介: 雷玉成，男，1962年出生，教授，博士研究生导师. 主要从事焊接工艺及设备、焊接过程控制及模拟、先进连接技术等方面的研究. 发表论文90余篇. Email：yclei@ujs.edu.cn

Properties of Sn-Ag-Cu lead free solders with different silver content

LIU Ping[1,2], GU Xiaolong[1], ZHAO Xinbing[2], LIU Xiaogang[1], ZHONG Haifeng[1] (1. Zhejiang Province Key Laboratory of Soldering & Brazing Materials and Technology, Zhejiang Metallurgical Research Institute, Hangzhou 310011, China; 2. Department of Materials Science and Engineering, Zhejiang University, Hangzhou 310027, China). pp 55 – 58

Abstract: The microstructure, melting behavior, mechanical properties, wettability and interfacial intermetallic compound (IMC) were studied on Sn-Ag-Cu (SAC) lead free solders with different Ag content (0.3, 1.0, 2.0, 3.0, 3.8wt%). The result indicates that SAC solders with higher Ag content present finer and denser IMC particles in the bulk solder, as a result of which the tensile strength of SAC solders increases with the increasing of Ag content, while the ductility decreases. The melting temperature of SAC305 and SAC387 solders was close to eutectic point as they have small melting temperature range. It was found that the wettability and interfacial IMC grain size of SAC0307/Cu joint are better than other tested solders.

Key words: Sn-Ag-Cu; lead-free solder; IMC; microstructure; melting temperature

Numerical simulation and experiments test of residual stress of longitudinal weld of thick SA508-3 steel pipe for nuclear power

CHI Luxin[1,2], MA Yonglin[2], XING Shuqing[2], CHEN Furong[2], CHEN Zhongyi[2] (1. College of Materials Science and Engineering, Chongqing University of Technology, Chongqing 400050, China; 2. College of Material and Metallurgy, Inner Mongolia University of Science and Technology, Baotou 014010, China). pp 59 – 62, 67

Abstract: Welding process of 60 mm thick SA508-3 steel pipe which is firstly used in nuclear power was simulated by ANSYS to obtain the temperature field and the residual stress. Simulated thermal and mechanical results were compared with the experimental results in the same welding parameters. It was found that the residual stress distribution is close to the measured values. During welding, the peak temperature exists in the centre of the heat source and its vicinity where the temperature gradient is much larger. However, the temperature descends sharply away from heat source. The residual stress on the outer surface of pipe are greater than that in the inner surface, of which the tensile residual stress in the welding zone and adjacent zone are largest, and gradually decreases away from the welding zone. The residual stress in the middle of cylinder is opposite to that in the two longitudinal ends. These results provide theoretical knowledge for the control of welding residual stress of pipe.

Key words: SA508-3 steel; residual stress; numerical simulation

Modeling and simulation for DE-GMAW

HUANG Jiankang[1], ZHU Ming[1], SHI Yu[1], ZHANG Yuming[2], Fan Ding[1] (1. Key Laboratory of Non-ferrous Metal Alloys and Processing, The Ministry of Education, Lanzhou University of Technology, Lanzhou 730050, China; 2. Center for Manufacturing, University of Kentucky, Lexington, KY 40506, USA). pp 63 – 67

Abstract: A dynamic mathematical model for welding arc was developed by adopting the method of equivalent current path according to the arc dynamic characteristics of DE-GMAW process and the rule of wire-melting. Based on that, simulations about non-consumable DE-GMAW and consumable DE-GMAW were carried out by MATLAB/Simulink. Then the influence of welding torches angle on stability of DE-GMAW process was simulated and analyzed. The results show that the developed mathematical model can reflect the DE-GMAW process well. When the angel between main and bypass torch is 45°, the response time for welding process to achieve stability is the shortest and is consistent with the actual welding process and the non-consumable DE-GMAW is much more stable than consumable DE-GMAW.

Key words: DE-GMAW; modelling; simulation

Analysis on low temperature toughness of self-shielded flux cored wire used for pipeline

SONG Shaopeng, LI Zhuoxin, LI Guodong, SHI Chuanwei (College of Materials Science and Engineering, Beijing University of Technology, Beijing 100124, China). pp 68 – 72

Abstract: Low temperature toughness of deposited metal made by three types self-shielded flux-cored wires used for X70 pipeline has been investigated, by analyzing macroscopic and SEM morphology of impact fracture, microstructure and statistics of inclusion. The results showed that low temperature toughness of deposited metal of three wires was significantly different. No. 3 wire has highest toughness with an impact absorbing energy average value of 330 J at –40 ℃, while the toughness of No. 1 wire is the lowest, whose impact absorbing energy average value is only 113 J at –30 ℃. Differences of inclusions and microstructure of deposited metal were the main reason for significantly different toughness. Uniform and fine equiaxed grains and small inclusions uniformly and dispersedly distributed in deposited metal are beneficial to improve the low temperature toughness.

Key words: self-shielded flux cored wire; inclusion; microstructure; low temperature toughness

Analysis of residual stress and hardness of T-joint on China low activation martensitic steel laser weld

LEI Yucheng[1], LI Zhennan[1], ZHU Yanshan[2], JU Xin[3] (1. School of Material Science and Engineering of Jiangsu University, Zhenjiang 212013, China; 2. Technical Center of Jinan Iron and Steel Co., Ltd., Jinan 250101, China; 3. Physics Department, University of Science and Technology of Beijing, Beijing 100083, China). pp 73 – 76

Abstract: T-joint of 4mm-thick CLAM steel was welded by 4 kW Nd: YAG laser welding equipment with different incident angles. Forming, distribution of residual stress and hardness are observed and analyzed. The result show that there is significant lack of fusion in the joint when the incidence angle is 14° and the joint fully fuses when the angle is 12° or 10° with the decreasing of incidence angle. The residual stress of the joint surface is compressive stress, the stress of flange is larger that of web when the angle is 12°. But the stress of web is larger when the angle is 10°. Inner stress largely changes in the section of the weld joint, compared with base metal, the hardness of weld zone has significantly increased and HAZ is not softened.

Key words: low activation martensitic steel; YAG laser welding; incidence angle; residual stress; hardness